

## Research Article

# Catalytic Dehydration of Ethanol over W/TiO<sub>2</sub> Catalysts Having Different Phases of Titania Support

Pongsatorn Kerdnoi<sup>1</sup>, Chaowat Autthanit<sup>1</sup>, Nithinart Chitpong<sup>2</sup>, Bunjerd Jongsomjit<sup>1,\*</sup><sup>1</sup>Center of Excellence on Catalysis and Catalytic Reaction Engineering, Department of Chemical Engineering, Faculty of Engineering, Chulalongkorn University, Bangkok 10330, Thailand.<sup>2</sup>Department of Textile Engineering, Faculty of Engineering, Rajamangala University of Technology Thanyaburi, Pathumthani 12110, Thailand.

Received: 15<sup>th</sup> August 2019; Revised: 4<sup>th</sup> October 2019; Accepted: 4<sup>th</sup> October 2019;  
Available online: 28<sup>th</sup> February 2020; Published regularly: April 2020

## Abstract

This study aims to investigate the catalytic behaviors on W/TiO<sub>2</sub> catalysts having different phases of TiO<sub>2</sub> towards catalytic dehydration of ethanol to higher value products including ethylene, diethyl ether, and acetaldehyde. In fact, TiO<sub>2</sub> support with different crystalline phases can result in differences of physico-chemical properties of the catalyst. Therefore, the present work reports on the catalytic behaviors that were altered with different phases of TiO<sub>2</sub> in catalytic ethanol dehydration to diethyl ether or ethylene as a major product. To prepare the catalysts, three different phases [anatase (A), rutile (R), and mixed phases (P25)] of TiO<sub>2</sub> supports were impregnated with 10 wt% of tungsten (W). It was found that the W/TiO<sub>2</sub>-P25 catalyst revealed higher activity among other catalysts. At 300 °C, all catalysts can produce the diethyl ether yield of 24.1%, 22.8%, and 10.6% for W/TiO<sub>2</sub>-P25, W/TiO<sub>2</sub>-A, and W/TiO<sub>2</sub>-R catalysts, respectively. However, when the reaction temperature was increased to 400°C, ethylene is the major product. The W/TiO<sub>2</sub>-P25 and W/TiO<sub>2</sub>-A catalysts render the ethylene yield of 60.3% and 46.2%, respectively, whereas only 15.9% is obtained from W/TiO<sub>2</sub>-R catalyst. The most important parameter influencing their catalytic properties appears to be the proper pore structure, acidity, and distribution of W species. Copyright © 2019 BCREC Group. All rights reserved

**Keywords:** Ethanol dehydration; Titania; Tungsten; Diethyl ether; Ethylene**How to Cite:** Kerdnoi, P., Autthanit, C., Chitpong, N., Jongsomjit, B. (2020). Catalytic Dehydration of Ethanol over W/TiO<sub>2</sub> Catalysts Having Different Phases of Titania Support. *Bulletin of Chemical Reaction Engineering & Catalysis*, 15(1): 96-103 (doi:10.9767/bcrec.15.1.5606.96-103)**Permalink/DOI:** <https://doi.org/10.9767/bcrec.15.1.5606.96-103>

## 1. Introduction

Currently, renewable energy resources such as solar, wind, and biomass have become an important way to achieve sustainable development. Increasing renewable energy consumption in the world can impact on the utilization of fossil fuel that is finite resources. When considered agricultural-based products or biomass, ethanol is one of the most important platform

chemicals, which can be derived from fermentation of biomass such as sugarcane, cassava, molasses, rice, corn, *etc.* [1]. In fact, ethanol can be converted into various valuable chemical compounds by catalytic dehydration and dehydrogenation of ethanol. The solid catalysts are preferred in these reactions. Ethanol dehydration typically includes two competitive routes to produce; (1) ethylene by endothermic reaction, and (2) diethyl ether by exothermic reaction. Therefore, the formation of ethylene favors at moderate to high temperatures (ca. 300-400 °C) to obtain high ethylene selectivity, while the for-

\* Corresponding Author.

E-mail: [bunjerd.j@chula.ac.th](mailto:bunjerd.j@chula.ac.th) (B. Jongsomjit);

Telp: +662-218-6874, Fax: 662-218-6877

mation of diethyl ether is prevail at lower temperatures (ca. 200-300 °C). Furthermore, these processes have many additional advantages, in particular the reduction of carbon dioxide (CO<sub>2</sub>) emissions, lower operating temperature, lower production costs and cleaner technology [2]. Ethylene product is widely used as raw materials in the manufacture of various polymers such as polyethylene, polyvinyl chloride, and polystyrene and other organic chemicals [3]. The diethyl ether product is commonly used as an extraction solvent. Moreover, diethyl ether has high cetane number and can be used in combination of petroleum fuel for gasoline and diesel engines [4,5]. In addition, acetaldehyde can be produced from ethanol dehydrogenation as a side reaction. Therefore, in order to obtain the desired products from ethanol, efficient catalysts must be developed and this becomes the most important factor of this research.

It is well known that the catalytic dehydration of ethanol has been investigated by using different catalysts in order to increase activity and lower the operation temperature. Normally, the solid acid catalysts containing alumina (Al<sub>2</sub>O<sub>3</sub>) and transition metal oxides such as zeolite, montmorillonite clays, silica (SiO<sub>2</sub>), zirconia (ZrO<sub>2</sub>), and titania (TiO<sub>2</sub>) are employed. However, they are presently expanded to include many catalysts, which are modified by adding other metals [6,7]. Among noble and transition metals, tungsten (W) is the most interesting choice since it is widely used. Moreover, W is an acidic catalytic material being highly active and selective for many reactions [8]. Phung et al. claimed that among the transition metal oxide catalysts, WO<sub>3</sub>/TiO<sub>2</sub> catalyst gave the highest catalyst activity for ethanol dehydration. It was discovered that the addition of W onto TiO<sub>2</sub> support gave higher activity at the low reaction temperature due to increased strong Brønsted acid sites for catalytic reaction [9]. Concerning the catalyst supports, it is well-known that TiO<sub>2</sub> exists in three different crystalline phase structures including anatase, rutile, and brookite. Anatase usually exhibits better activity than that of rutile and brookite. It is well known that TiO<sub>2</sub> in the form of anatase presents excellent properties for several catalytic systems involved in important thermos-catalytic processes including the NO<sub>x</sub> reduction with NH<sub>3</sub> and oil hydrodesulphurization. However, there are several reactions such as photocatalytic reactions for the unexpectedly high activity of rutile and brookite, which are accompanied by dramatic reduction of the specific surface area and pore volume [10-12]. Therefore, the different compositions of crystal-

line phases could exhibit the different physico-chemical properties and catalytic performance.

In this research work, W/TiO<sub>2</sub> catalysts were prepared by using TiO<sub>2</sub> supports having different phase compositions (anatase, rutile, and mixed phases). All catalysts were characterized by using various characterization techniques including inductively coupled plasma (ICP), X-ray diffraction (XRD), scanning electron microscope (SEM) and electron dispersive X-ray (EDX) spectroscopy, N<sub>2</sub>-physisorption and temperature-programed desorption of ammonia (NH<sub>3</sub>-TPD). Furthermore, the catalysts were tested in ethanol dehydration reaction under vapor phase of ethanol. To understand the catalytic behaviors of different TiO<sub>2</sub> phases, the effect of phase compositions in TiO<sub>2</sub> supports on the catalytic properties and product distribution were elucidated and discussed.

## **2. Materials and Method**

### **2.1 Preparation of Catalysts**

Three commercial phases of Titania (TiO<sub>2</sub>) were used as a support. Anatase (TiO<sub>2</sub>-A), rutile (TiO<sub>2</sub>-R), and P25 [TiO<sub>2</sub>-P25, consisting of anatase (~80%) and rutile (~20%)]. They were obtained from Sigma-Aldrich company. A precursor solution of tungsten was produced from ammonium metatungstate hydrate 99.99% trace metals basis [(NH<sub>4</sub>)<sub>6</sub>H<sub>2</sub>W<sub>12</sub>O<sub>40</sub>.4H<sub>2</sub>O] obtained from Sigma-Aldrich company and ethanol solution (99.99%) obtained from J.T. Baker company.

A tungsten content of 10 wt% was prepared by incipient wetness impregnation method onto the supports using a water solution of ammonium metatungstate. After impregnation, the catalyst samples were dried at 110 °C for 24 h and then calcined in air at 500 °C for 3 h (heating rate of 10 °C/min). The tungsten-containing on TiO<sub>2</sub> supports were denoted as W/TiO<sub>2</sub>-A, W/TiO<sub>2</sub>-R, and W/TiO<sub>2</sub>-P25.

### **2.2. Characterization**

Inductively coupled plasma (ICP): A quantity of elemental composition in the catalysts was measured by Perkin Elmer OPTIMA2000TM instrument. Before testing, sample must be converted to liquid form before testing by dissolving the sample in a concentrated sulfuric acid to produce a solution.

X-ray diffraction (XRD): The crystalline phases were identified by using a SIEMENS D-5000 X-ray diffractometer with Cu-Kα (λ = 1.54439 Å). The XRD patterns were recorded

over the  $2\theta$  between  $20^\circ$  and  $80^\circ$  with resolution of  $0.04^\circ$ .

**N<sub>2</sub>-physisorption (BET):** The adsorption-desorption isotherms of nitrogen at  $-196^\circ\text{C}$  were obtained from gas sorption techniques (Micromeritics ASAP 2020). The specific surface areas were determined from adsorption values for relative pressure ( $P/P_0$ ) by using the BET method. The total pore volume was estimated from the total amount of adsorbed nitrogen by using the BJH method. Scanning Electron Microscopy (SEM) and Energy Dispersive X-Ray Spectroscopy (EDX): The simple morphologies and elemental distribution were examined by SEM using a JEOL JSM-5800LV model and EDX using Link Isis series 300 program operated at 100 kV.

**Temperature-Programmed Desorption of ammonia (NH<sub>3</sub>-TPD):** The acid properties of obtained catalysts were investigated by NH<sub>3</sub>-TPD using Micromeritics Chemisorp 2750 Pulse Chemisorption System. In this experiment, the catalyst (50 mg) was evacuated with He at  $550^\circ\text{C}$ , and then NH<sub>3</sub> (gas) was adsorbed at  $100^\circ\text{C}$ . Finally, the NH<sub>3</sub>-TPD was performed by raising the temperature from  $50$  to  $500^\circ\text{C}$  to desorb ammonia, under a helium flow of  $40\text{ mL}\cdot\text{min}^{-1}$ , with a heating rate of  $10^\circ\text{C}\cdot\text{min}^{-1}$ . The amount of ammonia in effluent was measured via the thermal conductivity detector (TCD) as a function of temperature. The total acidity was calculated from the relation of TCD and temperature from  $50^\circ\text{C}$  to  $500^\circ\text{C}$ . After  $500^\circ\text{C}$ , the TPD peak was only decomposition of catalyst as proven by the TGA result.

**Thermo Gravimetric Analysis (TGA):** The thermal decomposition of TiO<sub>2</sub> supported catalysts were carried out from room temperature to  $1000^\circ\text{C}$  with a heating rate of  $10^\circ\text{C}/\text{min}$  un-

der nitrogen atmosphere using a STD Analyzer Model Q600 from TA instrument (USA).

### 2.3. Catalytic Reaction

The procedure used in carrying out the reactions was similar to those described by our previous work [13,14]. The catalytic ethanol dehydration was performed under atmospheric pressure in a fixed-bed flow microreactor. The catalyst (0.05 g) was charged onto packed quartz wool (0.01 g) in the middle of microreactor. In order to eliminate the impurity on surface of catalyst prior to reaction, the catalyst was pretreated in nitrogen with  $60\text{ mL}/\text{min}$  at  $200^\circ\text{C}$  for 1 h. Then, ethanol was vaporized and fed with controlled by a single syringe pump with at total flow rate of  $1.45\text{ mL}/\text{h}$  [i.e. the Weight Hourly Space Velocity (WHSV) =  $22.9\text{ h}^{-1}$ ]. Finally, all products were collected and analyzed at temperatures range from  $200^\circ\text{C}$  to  $400^\circ\text{C}$  under atmospheric pressure. The gaseous products were analyzed by a Shimadzu (GC-14B) gas chromatograph with flame ionization detector (FID) using capillary column (DB-5) at  $150^\circ\text{C}$ . Upon the reaction test, at least three times for each sampling were recorded. The average values for ethanol conversion and product distribution as a function of temperature were reported.

## 3. Results and Discussion

### 3.1. Catalyst Characterization

To identify the crystalline structure of the catalysts after W doping, the X-ray diffraction (XRD) was performed. The XRD patterns of TiO<sub>2</sub> supports and W/TiO<sub>2</sub> catalysts are illustrated in Figure 1. The results show that TiO<sub>2</sub>-A support displays the anatase peaks at  $25^\circ$  (major),  $37^\circ$ ,  $48^\circ$ ,  $54^\circ$ ,  $55^\circ$ , and  $62^\circ$ , whereas TiO<sub>2</sub>-R support exhibits rutile peaks at  $27^\circ$  (major),  $36^\circ$ , and  $55^\circ$  [11]. The diffraction pattern of TiO<sub>2</sub> matches well with the literature and were in good agreement with the standard spectra (JCPDS no.: 88-1175 and 84-1286). Moreover, TiO<sub>2</sub>-P25 support, which contains a mixture of anatase and rutile in an approximately 3:1 proportion, demonstrates both peaks of titania and anatase. The 10 wt% of W was impregnated onto three different titania supports and was observed W species with very low intensity peaks at  $22^\circ$  and  $33^\circ$ . The W/TiO<sub>2</sub>-A, W/TiO<sub>2</sub>-R, and W/TiO<sub>2</sub>-P25 catalysts show the similar XRD patterns as seen on those for the titania supports and also exhibits weaker intensity than that of the corresponding pure supports. This indicates that W was in

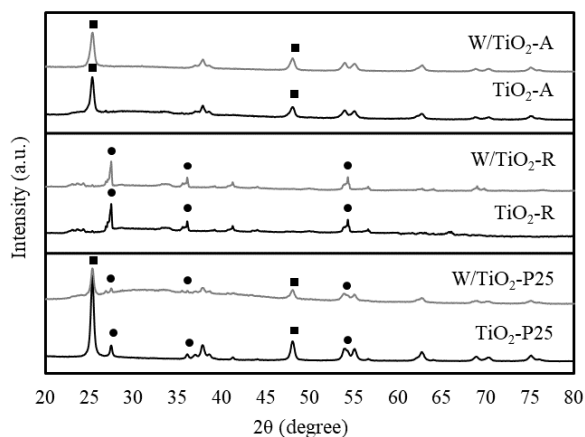


**Figure 1.** XRD patterns for all catalysts ( ■ anatase and ● rutile).

highly dispersed forms which cannot be detected by XRD technique. However, in case of W/TiO<sub>2</sub>-P25 catalyst, the peaks corresponding to anatase phase were significantly decreased due to the hindrance of strong intensity of XRD peaks for the anatase phase of titania [11,12]. According to the Scherrer equation,  $D = K\lambda C / \sin\theta$ , where  $\lambda$  is the wavelength ( $\lambda = 1.54056\text{\AA}$ ) and  $\theta$  is the Bragg angle, the crystallite sizes of all catalysts are shown in Table 1. It is suggested that the addition of W onto different phases of TiO<sub>2</sub> did not significantly affected the crystallite size of catalysts.

The textural properties, such as BET surface area, pore volume and pore diameter of TiO<sub>2</sub> supports and W/TiO<sub>2</sub> catalysts with different phases of TiO<sub>2</sub> determined by N<sub>2</sub> physisorption are reported in Table 1. The TiO<sub>2</sub>-A had a

significantly higher surface area (58 m<sup>2</sup>/g) and pore volume (0.24 cm<sup>3</sup>/g) relative to TiO<sub>2</sub>-R surface area (7 m<sup>2</sup>/g) and pore volume (0.01 cm<sup>3</sup>/g). Besides two pure phase supports, TiO<sub>2</sub>-P25 containing mostly anatase had similar surface area (47 m<sup>2</sup>/g) and pore volume (0.13 cm<sup>3</sup>/g) to TiO<sub>2</sub>-A. Moreover, W/TiO<sub>2</sub>-A and W/TiO<sub>2</sub>-P25 catalysts also exhibited higher surface areas and pore volume than that of W/TiO<sub>2</sub>-R catalyst. Therefore, the addition of tungsten onto titania supports only slightly changed the textural properties.

The N<sub>2</sub> adsorption-desorption isotherms at -196 °C for the catalysts with different phase of TiO<sub>2</sub> were conducted (not shown data). It was found that all supports and catalysts presented type IV adsorption isotherms with a H1 hysteresis loop at high relative pressure ( $0.7 < P/P_0$ )

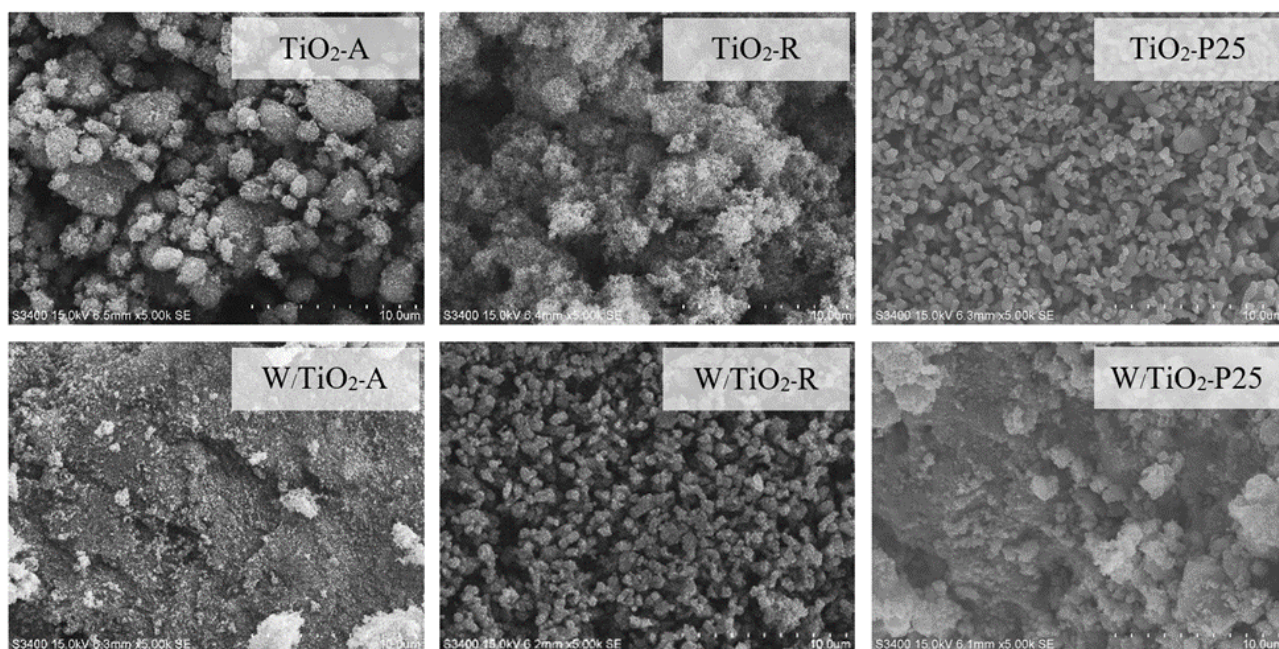


Figure 2. SEM micrographs of all catalysts.

Table 1. Characteristics of all supports and catalysts.

Catalysts	BET surface area, $S_{BET}$ (m <sup>2</sup> /g)	Pore volume (cm <sup>3</sup> /g)	Pore diameter (nm)	Total acidity ( $\mu\text{mol NH}_3/\text{g cat.}$ )	W content (wt%) <sup>a</sup>	W content (wt%) <sup>b</sup>	Crystallite size <sup>c</sup> (nm)
TiO <sub>2</sub> -A	58	0.24	11.9	1,639	-	-	16.9
W/TiO <sub>2</sub> -A	51	0.29	19.3	2,137	10.7	14.9	17
TiO <sub>2</sub> -R	7	0.01	10.7	75	-	-	16.7
W/TiO <sub>2</sub> -R	8	0.01	8.1	112	10.1	12	17.1
TiO <sub>2</sub> -P25	47	0.13	9.3	1,866	-	-	16.9
W/TiO <sub>2</sub> -P25	53	0.3	18.9	2,247	10.2	16.5	17.1

<sup>a</sup> obtained from ICP analysis

<sup>b</sup> obtained from EDX analysis

<sup>c</sup> obtained from XRD using the Scherrer equation



< 0.9) as defined by IUPAC classification, which confirm the mesoporosity of the catalysts. It can be realized that the hysteresis loop for both TiO<sub>2</sub>-A and TiO<sub>2</sub>-P25 supports are broader indicating larger pore volume than TiO<sub>2</sub>-R support. This result can be further confirmed by the corresponding pore volume, as shown in Table 1. It can be found that TiO<sub>2</sub>-A had larger pore volume (0.24 cm<sup>3</sup>/g) than that of other supports. Furthermore, the addition of tungsten onto titania supports can be slightly increased pore volume.

The surface acidity of the catalysts was measured by NH<sub>3</sub> temperature-programmed desorption (NH<sub>3</sub>-TPD) between 50 and 500 °C. Table 1 shows the number of acid site (total acidity) on catalysts calculated by integration of desorption areas of ammonia according to the Gauss curve fitting method. The TPD profiles (data not shown) for all catalysts related to the acid sites on the catalysts surface. The NH<sub>3</sub>-TPD profiles of TiO<sub>2</sub>-A, TiO<sub>2</sub>-P25, W/TiO<sub>2</sub>-A, and W/TiO<sub>2</sub>-P25 catalysts were found to have broad desorption peaks in range between 150 and 500°C, whereas TiO<sub>2</sub>-R and W/TiO<sub>2</sub>-R were not found any desorption peaks. TiO<sub>2</sub> supports (anatase, rutile and P25) present total acid site of 1639, 75 and 1866 μmol/g cat, respectively. After impregnation of W into all supports, all catalysts exhibited increased areas under TCD signal curve. It was found that W/TiO<sub>2</sub>-P25 catalyst had the highest amount of total acid sites of 2,247 μmol/g cat. It has been reported previously that the catalysts with higher acid site show good performance in alcohol dehydration (such as ethanol, methanol, butanol, etc.) leading to enhance the catalytic activity [14-16]. Therefore, the difference in catalytic behavior of all catalysts upon acidity is discussed further.

The morphologies and elemental distributions of titania supports having different phases were determined by using SEM and EDX as shown in Figures 2 and 3, respectively. The TiO<sub>2</sub> supports mostly exhibited irregular shape

of particles. The particles of W/TiO<sub>2</sub>-R catalyst were smaller than those of W/TiO<sub>2</sub>-A and W/TiO<sub>2</sub>-P25 catalysts (in form of catalyst patches). From the EDX mappings (Figure 3), it was found that titanium (Ti), oxygen (O) and tungsten (W) exhibited well distribution on the external surface of catalysts. Based on the EDX analysis, it can be observed that the amount of W being present in W/TiO<sub>2</sub>-P25 catalyst (16.5 wt%) was higher than that both in W/TiO<sub>2</sub>-A (14.9 wt%) and W/TiO<sub>2</sub>-R (12.0 wt%) catalysts as seen in Table 1. It was suggested that the presence of both phases (anatase and mixed phase) of titania support exhibited the high W content on the external surface of catalysts.

According to the results from ICP and EDX, it can be proposed that tungsten species had larger particle size than pore size of TiO<sub>2</sub> supports. The tungsten species were discovered on the external surface more than at the internal pore of catalysts. The amount of W was shown in Table 1. It was well known that the W concentrations at bulk (ICP) were ranged between 10.1-10.7 wt% for all W/TiO<sub>2</sub> based catalysts. However, the element concentration from the EDX analysis, which is not a bulk (but rather surface) analytical tool, gives information down to a depth of approximately 50 nm from the typical external granule. In addition, W ob-

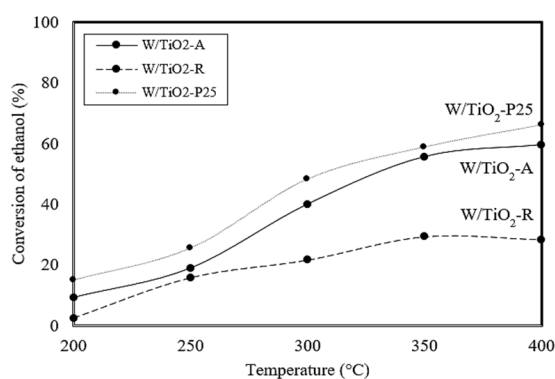


Figure 4. Ethanol conversion of all catalysts.

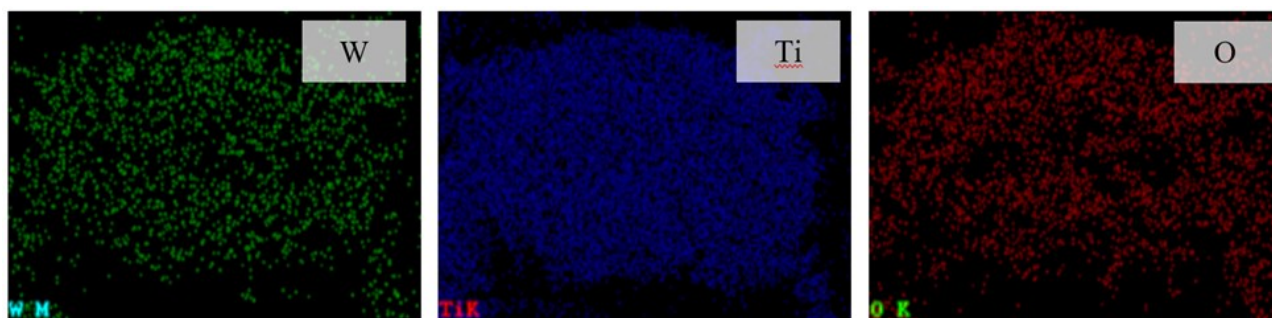


Figure 3. Typical EDX for W, Ti, and O mapping (W/TiO<sub>2</sub>-P25).

tained from EDX was higher than ICP measurement (12.0-16.5 wt%). This was due to the W accumulated mostly on the external surface of TiO<sub>2</sub> support.

### 3.2. Ethanol Dehydration Reaction

To measure the catalytic properties for W/TiO<sub>2</sub> catalysts having different phases of TiO<sub>2</sub>, the catalytic ethanol dehydration was performed at the reaction temperature range of 200 to 400 °C. The result of ethanol conversions is shown in Figure 4. It was found that ethanol conversion obviously increased with increasing the reaction temperatures for all catalysts, indicating no deactivation of catalysts up to 400 °C. The W/TiO<sub>2</sub>-P25 catalyst exhibited the highest ethanol conversion (66.2%) among other catalysts.

Considering the product distribution, the selectivity of ethylene is related to the reaction temperature as also described by many researchers [17-20]. The selectivity (in mol%) is defined as the molar ratio of a specific product to all products present (ethylene, acetaldehyde and diethyl ether). The reaction temperature is

usually a driving force to improve catalytic activity of endothermic reaction. As shown in Figure 5, it can be observed that ethylene selectivity increased with increasing reaction temperatures. The W/TiO<sub>2</sub>-P25 catalyst produced slightly higher ethylene selectivity than other catalysts. However, the formation of diethyl ether is favored by exothermic reaction, thus, increasing the reaction temperatures apparently resulted in decreasing diethyl ether selectivity based on the fact that diethyl ether is decomposed to ethylene at high temperature. At the low temperature (below 300 °C), W/TiO<sub>2</sub>-A and W/TiO<sub>2</sub>-P25 catalysts produced higher amount of diethyl ether than W/TiO<sub>2</sub>-R catalyst. Especially at 200 °C, W/TiO<sub>2</sub>-R catalyst did not produce any diethyl ether. Besides two products, acetaldehyde was well formed as a byproduct for W/TiO<sub>2</sub>-R catalyst.

A comparison of product yields of all supports and catalysts is shown in Table 2. The yield of each product is defined as ethanol conversion multiplies with their selectivity. For pure phases of TiO<sub>2</sub> support, it is obvious that the catalytic behaviors of W/TiO<sub>2</sub>-R and W/TiO<sub>2</sub>-A catalysts were similar to diethyl ether and ethylene yields due to good textural properties. All W/TiO<sub>2</sub> catalysts gave increased yield with increasing the reaction temperature up to 300 °C. In addition, at 300 °C, W/TiO<sub>2</sub>-P25 catalyst gave the highest diethyl ether yield (24.1%), whereas the highest ethylene yield (60.3%) of this catalyst was obtained at 400 °C.

Based on this study, it can be summarized that the phase composition of TiO<sub>2</sub> support can affect the catalytic behavior of W/TiO<sub>2</sub> catalysts. The mixed phases of TiO<sub>2</sub>-A and TiO<sub>2</sub>-R is more suitable for W probably due to its three major roles; (1) high surface area and (2) high amount of W species distributed on the exter-

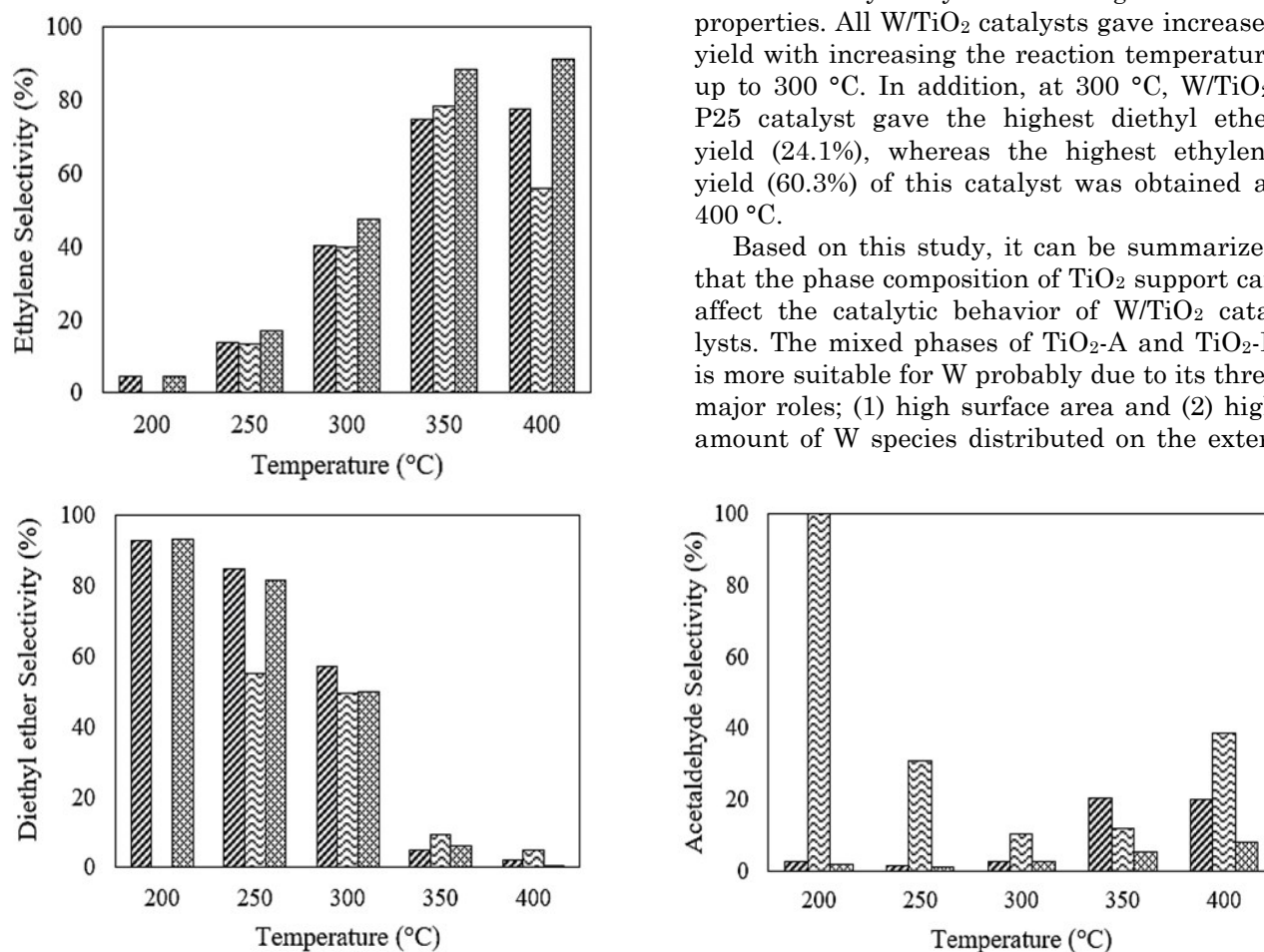


Figure 5. Selectivities of products for all catalysts ( W/TiO<sub>2</sub>-A, W/TiO<sub>2</sub>-R, W/TiO<sub>2</sub>-P25).

nal surface of catalyst and (3) introduce acid sites as active sites in the reaction. They were the factors leading to obtain higher activity for ethanol dehydration of the catalyst on mixed phase (P25) than other phases.

### 3.3. Thermal gravimetric analysis (TGA)

To determine the coke formation, the spent catalysts were analyzed by using TGA analysis. It can be concluded that TGA profiles of all spent catalysts using in the reaction exhibited similar activity (not shown data). At temperature higher than 200 °C, it was found that the addition of tungsten into TiO<sub>2</sub> catalysts promoted the coke formation due to the interaction between W and TiO<sub>2</sub> support introducing the

catalyst burning [21,22]. The amount of coke formation in spent catalysts were determined and reported in Table 3.

## 4. Conclusions

In this study, the results of W/TiO<sub>2</sub> supports having three different phases [anatase, rutile and mixed phases (P25)] with W loading constant (10 wt.%) was investigated by ethanol dehydration from the temperature range of 200 to 400 °C. The catalyst characterization was used to investigate the physico-chemical properties and acidity of W supported on TiO<sub>2</sub> catalysts. It reveals that W/TiO<sub>2</sub>-P25 catalyst was able to produce diethyl ether (24.1% yield) at 300 °C and ethylene (60.3% yield) at 400 °C. Besides the different phases of titania support, higher surface area of TiO<sub>2</sub> is likely to play an important role on the better dispersion of acid sites leading to increased catalytic activity. This catalyst can be potentially used as support for a catalyst in dehydration of ethanol to diethyl ether and ethylene.

## Acknowledgements

This research is funded by Chulalongkorn University and Cat-React industrial project.

## References

- [1] Sebayang, A., Masjuki, H., Ong, H.C., Dharma, S., Silitonga, A., Mahlia, T., Aditiya, H. (2016). A perspective on bioethanol production from biomass as alternative fuel for spark ignition engine, *RSC Adv.*, 6, 14964-14992.
- [2] Huber, G.W., Iborra, S., Corma A. (2006). Synthesis of transportation fuels from biomass: chemistry, catalysts, and engineering, *Chem. Rev.*, 106, 4044-4098.

**Table 3.** The amount of coke formation in the spent catalysts.

Catalyst	Temperature (°C)	Weight (%)	The amount of coke formation (%)
TiO <sub>2</sub> -A	200	99.88	0.56
	1000	99.32	
W/TiO <sub>2</sub> -A	200	99.59	8.74
	1000	90.89	
TiO <sub>2</sub> -R	200	99.94	0.49
	1000	99.45	
W/TiO <sub>2</sub> -R	200	99.96	1.18
	1000	98.78	
TiO <sub>2</sub> -P25	200	99.91	0.58
	1000	99.33	
W/TiO <sub>2</sub> -P25	200	99.51	4.71
	1000	94.82	

**Table 2.** Product yields of all catalysts.

Catalyst	Product Yield (%)	Temperature (°C)				
		200	250	300	350	400
W/TiO <sub>2</sub> -A	Ethylene	0.4	2.6	16.2	41.5	46.2
	Diethyl ether	8.5	16	22.8	2.7	1.3
	Acetaldehyde	0.3	0.3	1	11.3	12
W/TiO <sub>2</sub> -R	Ethylene	0	2.1	8.6	23	15.9
	Diethyl ether	0	8.7	10.6	2.8	1.5
	Acetaldehyde	2.4	4.9	2.3	3.5	11
W/TiO <sub>2</sub> -P25	Ethylene	0.7	4.4	22.9	52.1	60.3
	Diethyl ether	14	20.9	24.1	3.6	0.4
	Acetaldehyde	0.3	0.3	1.3	3.2	5.4

- [3] Soh, J.C., Chong, S.L., Hossain, S.S., Cheng, C.K. (2017). Catalytic ethylene production from ethanol dehydration over non-modified and phosphoric acid modified Zeolite HY (80) catalysts, *Fuel Process. Technol.*, 158, 85-95.
- [4] Alharbi, W., Brown, E., Kozhevnikova, E.F., Kozhevnikov, I.V. (2014). Dehydration of ethanol over heteropoly acid catalysts in the gas phase, *J. Catal.*, 319, 174-181.
- [5] Kamsuwan, T., Praserttham, P., Jongsomjit, B. (2017). Diethyl ether production during catalytic dehydration of ethanol over Ru- and Pt-modified H-beta zeolite catalysts, *J. Oleo Sci.*, 66, 199-207.
- [6] Lee, J., Szanyi, J., Kwak, J.H. (2017). Ethanol dehydration on  $\gamma$ -Al<sub>2</sub>O<sub>3</sub>: effects of partial pressure and temperature, *Mol. Catal.*, 434, 39-48.
- [7] Chen, B., Lu, J., Wu, L., Chao, Z. (2016). Dehydration of bio-ethanol to ethylene over iron exchanged HZSM-5, *Chinese J. Catal.*, 37, 1941-1948.
- [8] Onfroy, T., Clet, G., Bukallah, S.B., Visser, T., Houalla, M. (2006). Acidity of titania-supported tungsten or niobium oxide catalysts: correlation with catalytic activity, *Appl. Catal. A*, 298, 80-87.
- [9] Phung, T.K., Hernández, L.P., Busca, G. (2015). Conversion of ethanol over transition metal oxide catalysts: effect of tungsta addition on catalytic behaviour of titania and zirconia, *Appl. Catal. A*, 489, 180-187.
- [10] Jongsomjit, B., Wongsalee, T., Praserttham, P. (2005). Characteristics and catalytic properties of Co/TiO<sub>2</sub> for various rutile: anatase ratios, *Catal. Commun.*, 6, 705-710.
- [11] Jongsomjit, B., Wongsalee, T., Praserttham, P. (2005). Study of cobalt dispersion on titania consisting various rutile: anatase ratios, *Mater. Chem. Phys.*, 92, 572-577.
- [12] Kordouli, E., Dracopoulos, V., Vaimakis, T., Bourikas, K., Lycourghiotis, A., Kordulis, C. (2015). Comparative study of phase transition and textural changes upon calcination of two commercial titania samples: A pure anatase and a mixed anatase-rutile, *J. Solid State Chem.*, 232, 42-49.
- [13] Autthanit, C., Jongsomjit, B. (2018). Production of ethylene through ethanol dehydration on SBA-15 catalysts synthesized by sol-gel and one-step hydrothermal methods, *J. Oleo Sci.*, 67, 235-243.
- [14] Krutpijit, C., Jongsomjit, B. (2016). Catalytic ethanol dehydration over different acid-activated montmorillonite clays, *J. Oleo Sci.*, 65, 347-355.
- [15] Cecilia, J., García-Sancho, C., Mérida-Robles, J., Santamaría-González, J., Moreno-Tost, R., Maireles-Torres, P. (2015). V and V-P containing Zr-SBA-15 catalysts for dehydration of glycerol to acrolein, *Catal. Today*, 254, 43-52.
- [16] Akarmazyan, S.S., Panagiotopoulou, P., Kambolis, A., Papadopolou, C., Kondarides, D.I. (2014). Methanol dehydration to dimethylether over Al<sub>2</sub>O<sub>3</sub> catalysts, *Appl. Catal. B*, 145, 136-148.
- [17] Zhang, X., Wang, R., Yang, X., Zhang, F. (2008). Comparison of four catalysts in the catalytic dehydration of ethanol to ethylene, *Microporous Mesoporous Mater.*, 116, 210-215.
- [18] Zhan, N., Hu, Y., Li, H., Yu, D., Han, Y., Huang, H. (2010). Lanthanum-phosphorous modified HZSM-5 catalysts in dehydration of ethanol to ethylene: A comparative analysis, *Catal. Commun.*, 11, 633-637.
- [19] Limlamthong, M., Chitpong, N., Jongsomjit, B. (2019). Influence of Phosphoric Acid Modification on Catalytic Properties of  $\gamma$ -Al<sub>2</sub>O<sub>3</sub> Catalysts for Dehydration of Ethanol to Diethyl Ether, *Bull. Chem. React. Eng. Catal.*, 14, 1-8.
- [20] Autthanit, C., Praserttham, P., Jongsomjit, B. (2018). Oxidative and non-oxidative dehydrogenation of ethanol to acetaldehyde over different VO<sub>x</sub>/SBA-15 catalysts, *J. Environ. Chem. Eng.*, 6, 6516-6529.
- [21] Istadi, I., Anggoro, D.D., Amin, N.A.S., Ling, D.H.W. (2011). Catalyst deactivation simulation through carbon deposition in carbon dioxide reforming over Ni/CaO-Al<sub>2</sub>O<sub>3</sub> catalyst, *Bull. Chem. React. Eng. Catal.*, 6(2), 129-136.
- [22] Zhang, W., Qi, S., Pantaleo, G., Liotta, L.F. (2019). WO<sub>3</sub>-V<sub>2</sub>O<sub>5</sub> Active Oxides for NO<sub>x</sub> SCR by NH<sub>3</sub>: Preparation Methods, Catalysts' Composition, and Deactivation Mechanism - A Review, *Catalysts*, 9, 527-557.